Letters

A Parallel-Connected 24-Pulse Rectifier Using Hybrid Harmonic Reduction Method at DC Side

Yuxin Lian, Shiyan Yang, Hongqi Ben, Wei Bai, and Wei Yang, *Member, IEEE*

***Abstract*—This letter proposes a parallel-connected 24-pulse rectifier using a hybrid harmonic reduction method at the dc side. The proposed rectifier contains an unconventional interphase reactor (UIPR) with a double-tapped primary winding and secondary winding connected pulsewidth modulation converter. The proposed method is a combination of the passive and active harmonic method. From the viewpoint of total harmonic distortion (THD) of the input line current, ripple load voltage, and kilovoltampere rating of the active auxiliary circuit, the UIPR and active injecting current are optimally designed. An experimental prototype is developed to verify the theoretical analysis. The experimental THD is about 2.87%, which shows good performance of harmonic reduction.**

***Index Terms*—Hybrid harmonic reduction, interphase reactor (IPR), multipulse rectifier (MPR).**

I. Introduction

MULTIPULSE rectifier (MPR) is regarded as a preferred ac–dc converter in a high power rectification system because of its simple configuration and high reliability. Therefore, MPR is widely used in industrial application, such as vessel-integrated power system, aircraft converter system, adjustable speed driver, and electrochemical processes [1], [2]. However, as the important interface between the load and generator, the input line current total harmonic distortion (THD) of the traditional 12-pulse or 24-pulse rectifier fails to satisfy the requirement of the IEEE-519 standard [3].

According to lots of efforts that have been made to reduce the harmonics in the input line current, installing the passive or active devices at the dc side is one of the important methods [2]–[16]. The double-tapped interphase reactor (DIPR) is the representative of the passive method [6], [7]. In order to avoid the serious conduction losses problem when the tap number is more than 3, some researchers proposed unconventional IPR (UIPR) with secondary winding connecting a single-phase full-wave rectifier or a single-phase diode-bridge rectifier (DBR) [8]–[10]. Furthermore, by changing the primary winding tapped number of UIPR with optimal design, the 12-pulse rectifier can perform as a 36-pulse or 48-pulse rectifier [10]. A simple 18-pulse star rectifier combing a double-star rectifier and four-tapped interphase reactor (IPR) with four diodes has been proposed recently, which increases the pulse number of the load voltage and step number of the input line current [3]. In addition, another new method is using two auxiliary diodes installed between the two retrofitted DIPRs to achieve input current step doubling for a 12-pulse rectifier [11].

The active method combines active devices and pulsewidth modulation (PWM) technology by generating a particular injection current to modulate the output currents of the three-phase DBRs [12]–[16]. The active methods can be divided into separate modulation methods and unified modulation methods, according to the modulation characteristics of the active auxiliary circuits. The separate modulation methods do not require IPR by installing an auxiliary circuit on the output side of each rectifier bridge. The unified modulation methods require IPR to provide a common conduction path for modulation current. The effect of the unified method is obvious and the input current is close to the sine wave.

In general, the passive methods can increase the pulse number of load voltage and the step number of input current simultaneously while cannot totally eliminate higher harmonics. The active methods have better harmonic reduction effects, while the control and drive circuits are complicated compared with passive methods. Therefore, combining the advantages of active and passive methods, a hybrid harmonic reduction method is proposed to provide a new solution to deal with power quality on both ac and dc side, and a novel parallel-connected 24-pulse rectifier is obtained. After using the proposed method, the experimental THD of the input line current is about 2.87%, which can easily meet the increasingly stringent requirements for aviation or aerospace applications.

II. Circuit Configuration of the Proposed Rectifier

A. Circuit Configuration

Fig. 1 shows the proposed rectifier using the hybrid harmonic reduction method. The main circuit is identical to the conventional parallel-connected 12-pulse diode rectifier with

Manuscript received 22 March 2022; revised 23 April 2022; accepted 10 May 2022. Date of publication 19 May 2022; date of current version 26 July 2022. This work was supported by the National Natural Science Foundation of China under Grant 51677036. *(Corresponding author: Wei Yang.)*

The authors are with the School of Electrical Engineering and Automation, Harbin Institute of Technology, Harbin 150001, China (e-mail: lianyx@hit.edu.cn; syyang@hit.edu.cn; benhq@hit.edu.cn; 907845373@qq.com; yangv@hit.edu.cn).

Color versions of one or more figures in this article are available at https://doi.org/10.1109/TPEL.2022.3175571.

Digital Object Identifier 10.1109/TPEL.2022.3175571

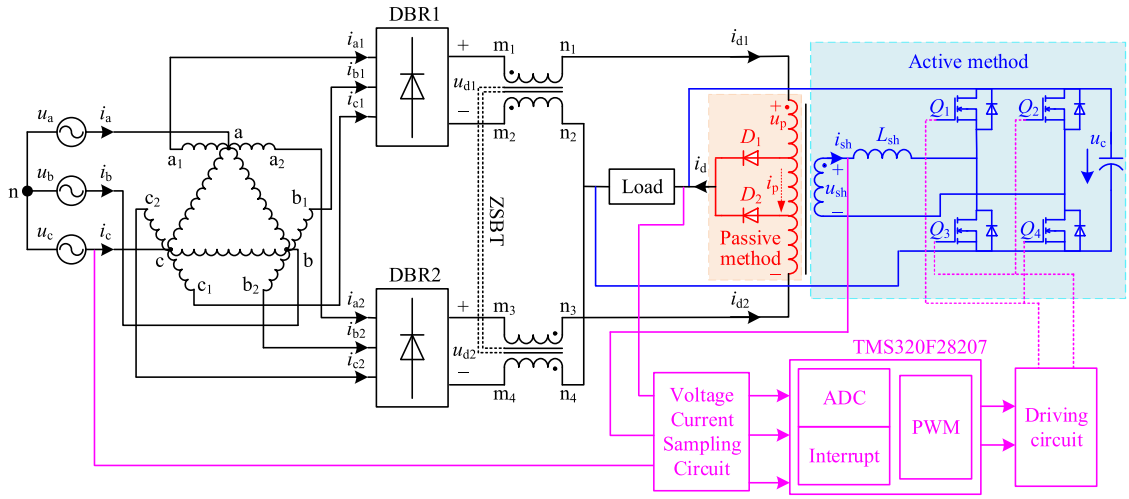

Fig. 1. Proposed rectifier using the hybrid harmonic reduction method.

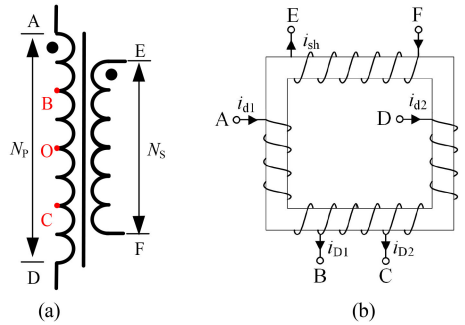

Fig. 2. Configurations of UIPR. (a) Tap structure. (b) Winding configuration.

the exception of a UIPR with a double-tapped primary winding and secondary winding connected PWM converter. The delta-connected autotransformer and zero-sequence blocking transformer are consistent with the description in the pieces of literature [8] and [10]. The primary winding of the UIPR connects two diodes operating as the passive harmonic reduction. The secondary winding and the single-phase bridge PWM converter comprise the active harmonic reduction, which generates a particular injecting current. The tap structure and winding configuration of the UIPR are shown in Fig. 2(a) and (b), respectively. Turn ratio m is defined as secondary winding N_s to the primary winding N_p. Assume that the turn ratio m is equal to 1. The tap ratio α is defined as

$$\alpha = \frac{N_{OB}}{N_P} = \frac{N_{OC}}{N_P}. \tag{1}$$

B. Operation Modes of UIPR

The operation modes of UIPR are determined by the output voltage of DBRs and active injection current. Assume that the output voltages of DBR1 and DBR2 are u_{d1} and u_{d2}, respectively, and the active injection current is i_{sh}. From the relation among u_{d1}, u_{d2}, and i_{sh}, there are four operation modes, which are as follows.

1) *Mode I*: When $u_{d1}>u_{d2}$ and $i_{sh}=0$, the UIPR operates under mode I as the conventional DIPR. In this mode, diode D_1 of the primary winding is forward biased and ON, and diode D_2 is reverse biased and OFF. According to the ampere-turn principle and Kirchhoff's voltage law, the output currents i_{d1} and i_{d2} of the DBRs, and the hybrid modulation current of primary winding i_p are as follows:

$$\begin{cases} (0.5-\alpha)i_{d1} = (0.5+\alpha)i_{d2} \\ i_p = 0.5(i_{d1}-i_{d2}). \end{cases} \tag{2}$$

The load voltage is expressed as

$$u_d = u_{d1} - (0.5-\alpha)(u_{d1}-u_{d2}). \tag{3}$$

2) *Mode II*: When $u_{d1}<u_{d2}$ and $i_{sh}=0$, the UIPR operates under mode II as the conventional DIPR. In this mode, diode D_2 is forward biased and ON, and diode D_1 is reverse biased and OFF. Similarly, the relation among i_{d1}, i_{d2}, and i_p is

$$\begin{cases} (0.5+\alpha)i_{d1} = (0.5-\alpha)i_{d2} \\ i_p = 0.5(i_{d1}-i_{d2}). \end{cases} \tag{4}$$

The load voltage u_d is calculated as

$$u_d = u_{d1} - (0.5+\alpha)(u_{d1}-u_{d2}). \tag{5}$$

3) *Mode III:* When $u_{d1}>u_{d2}$ and $i_{sh}\neq 0$, the UIPR operates under mode III. In this mode, diode D_1 is forward biased and ON, and diode D_2 is OFF. The load voltage is similar to mode I. The current i_p is affected by the active injection current i_{sh}. Therefore, the relation among i_{d1}, i_{d2}, and i_p is

$$\begin{cases} (0.5-\alpha)i_{d1} = (0.5+\alpha)i_{d2} \\ i_p = 0.5(i_{d1}-i_{d2}) + i_{sh}/m. \end{cases} \tag{6}$$

4) *Mode IV*: When $u_{d1}<u_{d2}$ and $i_{sh}\neq 0$, the UIPR operates under mode IV. In this mode, diode D_2 is forward biased and ON, and diode D_1 is OFF. The load voltage is similar

to mode II. Similarly, the relation among i_{d1}, i_{d2}, and i_p is

$$\begin{cases} (0.5+\alpha)i_{d1} = (0.5-\alpha)i_{d2} \\ i_p = 0.5(i_{d1}-i_{d2}) + i_{sh}/m. \end{cases} \tag{7}$$

From the above analysis, the output current of the DBRs and the hybrid modulation current are different in different operation modes.

III. Hybrid Modulation Current Strategy

According to the operation modes of UIPR, the rectifier operates as a 24-pulse rectifier based on the conventional DIPR in mode I and mode II. Assume that the current through the primary winding of UIPR is inherent modulation current i_{pm}. The input current THD of the rectifier is determined by i_{pm}, i_{sh}, α, and m.

A. Inherent Modulation Current

Assume that the load of the proposed rectifier is a large inductance loading and the load current i_d can be viewed as a constant I_d. The inherent modulation current is similar with the circulating current of the well-known DIPR, as discussed in [6]–[8]. Therefore, the inherent modulation current i_{pm} meets

$$i_{pm} = (S_p - S_q)\alpha I_d \tag{8}$$

where S_p and S_q are the switching functions of diodes D_1 and D_2, respectively.

B. Optimal Modulation Current Matching Strategy

Assume that the objective is to eliminate all harmonic components of the input current of the rectifier.

Thus, the input current should meet the ideal condition as follows:

$$\begin{cases} i_a = I_E \sin(\omega t) \\ i_b = I_E \sin(\omega t - 2\pi/3) \\ i_c = I_E \sin(\omega t + 2\pi/3) \end{cases} \tag{9}$$

where I_E is the amplitude of the input current.

According to the symmetry of the proposed rectifier, the output currents i_{d1} and i_{d2} of the DBRs can be expressed as

$$\begin{cases} i_{d1} = 0.5I_d + i_{pu} \\ i_{d2} = 0.5I_d - i_{pu} \end{cases} \tag{10}$$

where i_{pu} is the ideal modulation current.

The ideal modulation current is a symmetrical triangle of six times the source frequency, which has been derived in [10] and [11]. Therefore, the modulation current waveforms can be obtained by the software of Mathcad, as shown in Fig. 3. In Fig. 3, h_1 and w_1 are the height and width of the compensation triangle, and h_2 and w_2 are the height and width of the inherent passive modulation current. Parameters h_1, w_1, h_2, and w_2 are determined by the tap ratio of UIPR. If the injection current generated by the active auxiliary circuit exactly compensates the inherent passive modulation current, the input current waveform is approximately the standard sine wave, and the THD value is about 1.06%. Although the effect is optimal, it is difficult to achieve because of the steep rise and drop of the active injection current waveform.

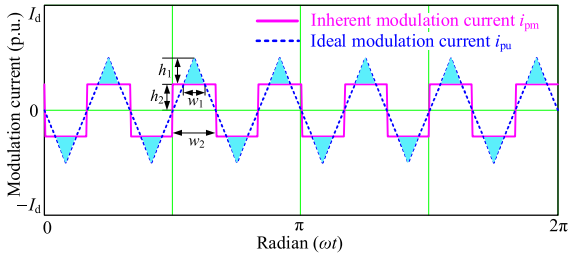

Fig. 3. Hybrid modulation current.

The optimal modulation current matching strategy partially compensates the amplitude part of the inherent passive modulated current, as shown in the shaded part in Fig. 3. Assume that the height coefficient of the compensation triangle is k_w and the width coefficient is k_h, which are defined as the ratio of the actual value to the h_1 and w_2, respectively. Furthermore, the active injection current can be expressed as

$$i_{sh} = \begin{cases} 0, \omega t \in [\frac{k\pi}{3}, \frac{k\pi}{3} + \frac{\pi}{12} - \frac{k_h\pi}{12}] \\ (\alpha - 0.5)k_w I_d \left[\frac{12}{k_h\pi}(\omega t - \frac{k\pi}{3}) + 1 - \frac{1}{k_h}\right], \\ \omega t \in [\frac{k\pi}{3} + \frac{\pi}{12} - \frac{k_h\pi}{12}, \frac{k\pi}{3} + \frac{\pi}{12}] \\ (0.5 - \alpha)k_w I_d \left[\frac{12}{k_h\pi}(\omega t - \frac{k\pi}{3}) - 1 - \frac{1}{k_h}\right], \\ \omega t \in [\frac{k\pi}{3} + \frac{\pi}{12}, \frac{k\pi}{3} + \frac{\pi}{12} + \frac{k_h\pi}{12}] \\ 0, \omega t \in [\frac{k\pi}{3} + \frac{\pi}{12} + \frac{k_h\pi}{12}, \frac{k\pi}{3} + \frac{\pi}{4} - \frac{k_h\pi}{12}] \\ (0.5 - \alpha)k_w I_d \left[\frac{12}{k_h\pi}(\omega t - \frac{k\pi}{3}) + 1 - \frac{3}{k_h}\right], \\ \omega t \in [\frac{k\pi}{3} + \frac{\pi}{4} - \frac{k_h\pi}{12}, \frac{k\pi}{3} + \frac{\pi}{4}] \\ (\alpha - 0.5)k_w I_d \left[\frac{12}{k_h\pi}(\omega t - \frac{k\pi}{3}) - 1 - \frac{3}{k_h}\right], \\ \omega t \in [\frac{k\pi}{3} + \frac{\pi}{4}, \frac{k\pi}{3} + \frac{\pi}{4} + \frac{k_h\pi}{12}] \\ 0, \omega t \in [\frac{k\pi}{3} + \frac{\pi}{4} + \frac{k_h\pi}{12}, \frac{k\pi}{3} + \frac{\pi}{3}] \end{cases} \tag{11}$$

where k is the natural number.

From the viewpoint of THD of the input line current, ripple voltage of the load, and kilovoltampere (KVA) rating of the active auxiliary circuit, the UIPR and active injecting current are optimally designed. The load voltage and the voltage across the secondary winding of UIPR have been derived in [8] and [10].

It is preferred to determine the value range of tap ratio through load voltage. Then, the width and height coefficients of active injection current are changed, respectively, in the above range. Thus, the variation rule of THD of input current and KVA of the active auxiliary circuit is obtained, respectively. Finally, under multiobjective constraints, the optimal values of the above three parameters are obtained as follows:

$$\begin{cases} k_w = 1 \\ k_h = \frac{3(\sqrt{6}-\sqrt{2}+1)}{16} \\ \alpha = 0.19. \end{cases} \tag{12}$$

Fig. 4 shows variation in the THD of input current and KVA of the active auxiliary circuit, respectively, for different parameters when α is equal to 0.19. Under the optimal parameters, the THD

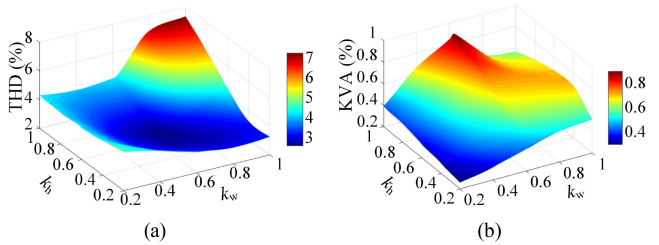

Fig. 4. Variation in THD and KVA for different parameters k_w and k_h. (a) THD of input current. (b) KVA of the active auxiliary circuit.

is 3.64%, the KVA is 0.9%, and the ripple coefficient of the load voltage is 0.064.

C. Analysis of Active Auxiliary Circuit

The topology of the active auxiliary circuit is a single-phase bridge PWM converter. The PWM converter adopts bipolar modulation mode and operates in rectification and inverter state. In order to ensure the normal operation of the active auxiliary circuit, it is necessary to design the input inductor, dc side capacitance, and control circuit. The input inductor L_{sh} affects the tracking speed and ripple of the active injection current. The maximum value and the minimum value of L_{sh} are determined according to the slope and ripple requirements of the inductor current in each switching period. From (11), the slope of the active injection current can be expressed as

$$k_{sh} = \frac{24k_w}{k_h T} |\alpha - 0.5| I_d \tag{13}$$

where T is the input voltage cycle.

According to the operation principle of a single-phase bridge PWM converter, the minimum slope of the inductor current is

$$k_{Lsh\,\min} = \left(\frac{di_L}{dt}\right)_{\min} = \frac{(U_C - u_{sh})_{\min}}{L_{sh}}. \tag{14}$$

In order to ensure the tracking speed of the active injection current, the minimum slope of the inductance current in each switching cycle is required to be greater than the slope of the active injection current. According to (13) and (14), the maximum value of the input inductor L_{sh} meets

$$L_{sh\,\max} < \frac{k_h T (U_C - u_{sh})_{\min}}{24k_w |\alpha - 0.5| I_d}. \tag{15}$$

In addition, in order to reduce the current ripple of the input inductor, the minimum value of the input inductor should meet

$$L_{sh\,\min} > \frac{(U_C - u_{sh})_{\min}}{2\Delta i_{Lsh} f_s} \tag{16}$$

where Δi_{Lsh} is the current ripple, and f_s is the switching frequency.

Assume that the input voltages of the proposed rectifier are

$$\begin{cases} u_a = \sqrt{2}E\sin(\omega t) \\ u_b = \sqrt{2}E\left(\omega t - 2\pi/3\right) \\ u_c = \sqrt{2}E\left(\omega t + 2\pi/3\right) \end{cases} \tag{17}$$

where E is the rms value of input voltage.

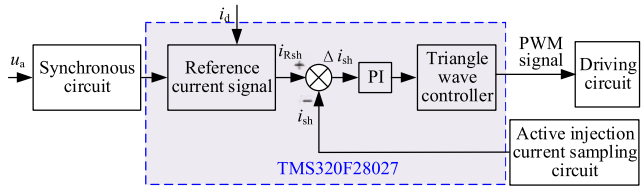

Fig. 5. Control block of the single-phase bridge PWM converter.

TABLE I
RECTIFIER SPECIFICATIONS AND COMPONENTS FOR EXPERIMENT

Parameter	Value
Input phase voltage (rms)	115V
Line frequency	50Hz
Load resistance	30Ω
Load filtering inductance	10mH
Primary-tapped ratio (α) of the UIPR	0.1875
Turn ratio (m) of the UIPR	1
Rated output power	3kW
Switching frequency of PWM converter	60kHz
Output voltage of PWM converter	300V

As discussed in [6], the critical inductance value of the UIPR can be presented by (17)

$$L_B = \frac{\alpha_s E}{\omega I_{d\,\min}(1 - 2\alpha)}\left(2\sqrt{3} - 2 - \sqrt{2}\right) \tag{18}$$

where α_s is the ratio of the output voltages of delta-connected autotransformer to the input voltage, and α_s is equal to be $(\sqrt{6} - \sqrt{2})$, as discussed in [10].

As the turn ratio of the UIPR is equal to 1, the inductance value of secondary winding is the same as (18). Therefore, when designing the input inductor of a single-phase bridge PWM converter, the effect of leakage inductance of UIPR should be considered comprehensively.

To select the output capacitance of the dc side, refer to the following empirical formula:

$$C > \frac{u_{sh} i_{sh} \cos\varphi_C}{2\omega_C U_C \Delta u_C} \tag{19}$$

where φ_C is the phase difference between the input voltage and current of the single-phase bridge PWM converter, ω_C is the angular frequency of the input voltage of the converter, and Δu_C is the ripple of the output voltage.

Fig. 5 shows the control block of the single-phase bridge PWM converter, which adopts the current single-loop control based on DSP TMS320F28027. The control circuit mainly includes power grid voltage sampling circuit, load current sampling circuit, UIPR secondary winding current sampling circuit, and driving circuit.

IV. EXPERIMENTAL VALIDATION

In order to validate the aforementioned analysis, an experimental setup using the hybrid harmonic reduction method is designed. Table I presents the rectifier specifications and components, and Fig. 6 shows the photograph of the partial experimental setup. The input of the experimental setup is from Chroma programmable ac source 61702. The experimental results are

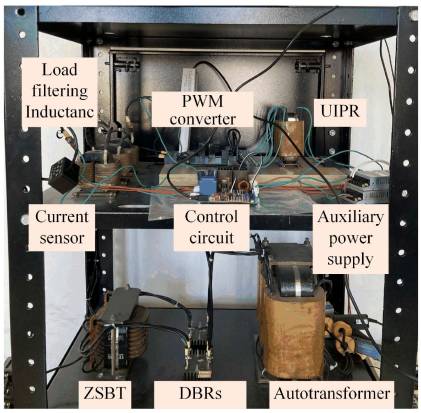

Fig. 6. Photograph of the partial experimental setup.

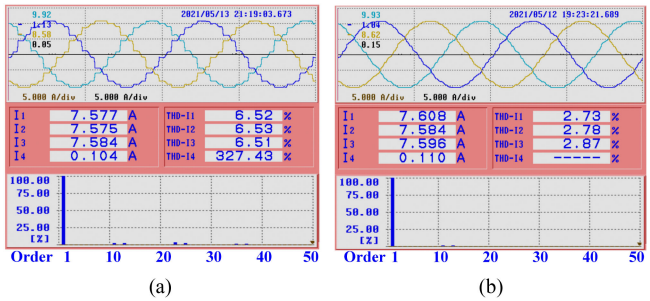

Fig. 7. Input line currents and their spectrum. (a) Without an active injection current. (b) Using hybrid harmonic reduction method.

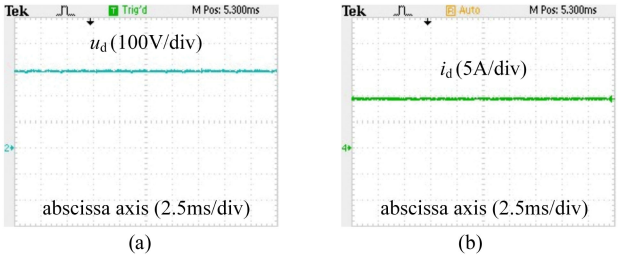

Fig. 8. Load voltage and load current before active injection current is added. (a) Load voltage. (b) Load current.

measured by the Tektronix TPS2024B oscilloscope. The THD and frequency spectrum of input current are measured by HIOKI 3196 power quality analyzer.

Fig. 7(a) shows the input line currents and their spectrum of the proposed rectifier without active injection current, and the UIPR operates as the conventional DIPR with a passive harmonic reduction method. Fig. 7(b) shows the input line currents and their spectrum using the hybrid harmonic reduction method under optimal parameters. The experimental values of THD are less than that of the theoretical value due to the filtering of leakage inductance of autotransformer and UIPR. Compared with Fig. 7(a), the hybrid harmonic reduction method is effective in reducing harmonic distortion of input currents.

Figs. 8 and 9 show the load voltage and load current before and after the active injection current is added. The load voltage and load current are smoothed by the load filtering inductor, and they are approximately constant. In addition, compared with Fig. 8,

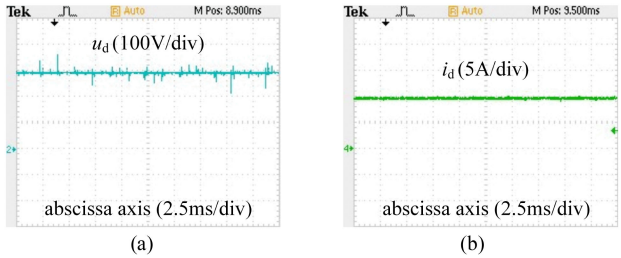

Fig. 9. Load voltage and load current after active injection current is added. (a) Load voltage. (b) Load current.

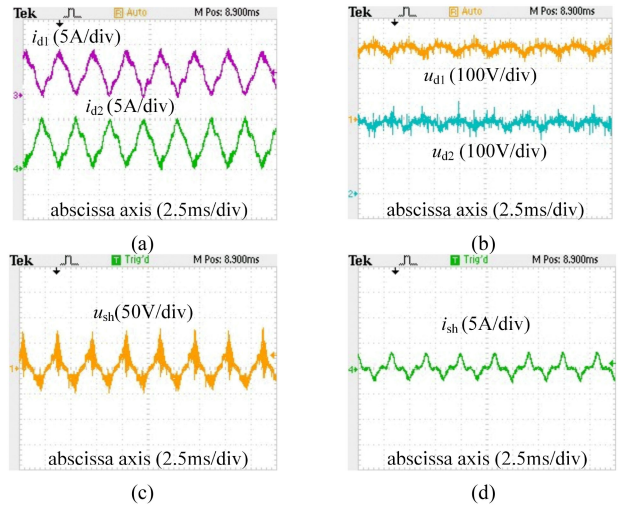

Fig. 10. Measured waveforms of the proposed rectifier. (a) Output currents i_{d1} and i_{d2} of DBRs. (b) Output voltages u_{d1} and u_{d2} of DBRs. (c) Voltage u_{sh} across the secondary winding of UIPR. (d) Active injection current i_{sh}.

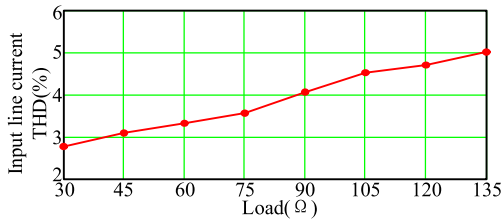

Fig. 11. Input line current THD under different load resistances.

the load voltage waveform in Fig. 9 has significant interference due to the active auxiliary circuit.

Fig. 10 shows the measured waveforms of the proposed rectifier. Fig. 10(a) and (b) shows the output currents and voltage of DBRs separately. Fig. 10(c) shows the voltage u_{sh} across the secondary winding of UIPR. Fig. 10(d) shows the active injection current i_{sh}. The currents i_{d1} and i_{d2} are modulated obviously when the active injection current with optimal parameters. Consequently, the input currents of the DBRs are also changed and the input current of the rectifier is modulated near sinusoidal.

Fig. 11 shows the input line current THD under the different load resistances. In Fig. 11, the THD is less than 5% in a wide range of load and it could meet the requirement of most industrial applications.

TABLE II
COMPARISON WITH THE SIMILAR RECTIFIER TOPOLOGIES

Indicators	24-pulse rectifier [6]	24-pulse rectifier [9]	24-pulse rectifier [11]	12-pulse rectifier [13]	12-pulse rectifier [15]	Proposed rectifier
Input current THD	7.52%	7.52%	7.52%	3.1%	1.3%	3.64%
Efficiency	96.89%	97.75%	97.31%	93.7%	97.7%	96.53%
Structure of IPR	DIPR	UIPR	Two retrofitted DIPR	secondary winding with auxiliary circuit	secondary winding with auxiliary circuit	Double tap and secondary winding
KVA rating of IPR	1.65%	3.11%	6.3%	3.1%	3.1%	2.28%
KVA rating of active auxiliary circuit	—	—	—	2.27%	2%	0.9%
Complexity	Simple	Simple	Slightly complicated	Slightly complicated	complicated	Slightly complicated

In addition, to clarify the weaknesses and strengths of the proposed rectifier, Table II presents the comparison results with similar rectifiers proposed in [6], [9], [11], [13], and [15]. Compared with the 24-pulse rectifiers using the passive harmonic reduction method, although the complexity is slightly increased, the input current THD is reduced from 7.52% to 3.64% and the experimental result is about 2.87%. The proposed rectifier has a stronger harmonic reduction ability. Compared with the 12-pulse rectifier using the active harmonic reduction method, although the input current THD is increased, the KVA rating of IPR and active auxiliary circuit is deceased.

V. CONCLUSION

This letter proposed a parallel-connected 24-pulse rectifier using a hybrid harmonic reduction method at the dc side. The proposed method is based on UIPR with a double-tapped primary winding and secondary winding connected active auxiliary circuit. By analyzing the hybrid modulation current matching strategy, the tap ratio of UIPR and active injection current is optimally designed from the viewpoint of THD of the input line current, ripple load voltage, and KVA of the active auxiliary circuit. Theoretical analysis and experimental results verify the effectiveness of the proposed method. The experimental THD of the input line current is about 2.87%. Compared with the rectifier based on DIPR not using the hybrid harmonic reduction method, the harmonic reduction ability of the proposed rectifier is improved significantly.

REFERENCES

[1] B. Singh, S. Gairola, B. N. Singh, A. Chandra, and K. Al-Haddad, "Multipulse AC-DC converters for improving power quality: A review," *IEEE Trans. Power Electron.*, vol. 23, no. 1, pp. 260–281, Jan. 2008.

[2] Q. Du, L. Gao, Q. Li, T. Li, and F. Meng, "Harmonic reduction methods at DC side of parallel-connected multipulse rectifiers: A review," *IEEE Trans. Power Electron.*, vol. 36, no. 3, pp. 2768–2782, Mar. 2021.

[3] M. A. Malek and M. A. G. Khan, "A simple 18-pulse star rectifier using two passive auxiliary circuits at DC link," *IEEE Trans. Power Electron.*, vol. 37, no. 5, pp. 5583–5593, May 2022.

[4] J. Chen, H. Bai, J. Chen, and C. Gong, "A novel parallel configured 48-pulse autotransformer rectifier for aviation application," *IEEE Trans. Power Electron.*, vol. 37, no. 2, pp. 2125–2138, Feb. 2022.

[5] R. Abdollahi and G. B. Gharehpetian, "Inclusive design and implementation of novel 40-pulse ac-dc converter for retrofit applications and harmonic mitigation," *IEEE Trans. Ind. Electron.*, vol. 63, no. 2, pp. 667–677, Feb. 2016.

[6] S. Yang, F. Meng, and W. Yang, "Optimum design of interphase reactor with double-tap changer applied to multipulse diode rectifier," *IEEE Trans. Ind. Electron.*, vol. 57, no. 9, pp. 3022–3029, Sep. 2010.

[7] S. Choi, B. S. Lee, and P. N. Enjeti, "New 24-pulse diode rectifier systems for utility interface of high-power AC motor drives," *IEEE Trans. Ind. Appl.,* vol. 33, no. 2, pp. 531–541, Mar./Apr. 1997.

[8] Y. Lian, S. Yang, K. Xu, Y. Li, and W. Yang, "Harmonic reduction mechanism at DC link of two different 24-pulse rectifiers," in *Proc. IEEE Transp. Electrific. Conf. Expo, Asia-Pacific*, Aug. 2017, pp. 1–6.

[9] S. Yang, J. Wang, and W. Yang, "A novel 24-pulse diode rectifier with an auxiliary single-phase full-wave rectifier at DC side," *IEEE Trans. Power Electron.*, vol. 32, no. 3, pp. 1885–1893, Mar. 2017.

[10] Y. Lian, S. Yang, and W. Yang, "Optimum design of 48-pulse rectifier using unconventional interphase reactor," *IEEE Access*, vol. 7, pp. 61240–61250, 2019.

[11] J. Wang, A. Chen, X. Yao, Q. Guan, and Q. Chen, "Input current step-doubling for autotransformer-based 12-pulse rectifier using two auxiliary diodes," *IEEE Trans. Ind. Electron.*, vol. 69, no. 8, pp. 7607–7617, Aug. 2022.

[12] F. Meng, X. Xu, L. Gao, and C. Cai, "Active harmonic reduction using DC-side current injection applied in a novel large current rectifier based on fork-connected autotransformer," *IEEE Trans. Ind. Electron.*, vol. 64, no. 7, pp. 5250–5264, Jul. 2017.

[13] V. Sheelvant, R. Kalpana, B. Singh, and P. P. Saravana, "Improvement in harmonic reduction of a zigzag autoconnected transformer based 12-pulse diode bridge rectifier by current injection at DC side," *IEEE Trans. Ind. Appl.,* vol. 53, no. 6, pp. 5634–5644, Nov./Dec. 2017.

[14] A. de Oliveira Costa Neto, A. L. Soares, G. B. de Lima, D. B. Rodrigues, E. A. A. Coelho, and L. C. G. Freitas, "Optimized 12-pulse rectifier with generalized delta connection autotransformer and isolated SEPIC converters for sinusoidal input line current imposition," *IEEE Trans. Power Electron.*, vol. 34, no. 4, pp. 3204–3213, Apr. 2019.

[15] F. Meng, W. Yang, S. Yang, and L. Gao, "Active harmonic reduction for 12-pulse diode bridge rectifier at DC side with two-stage auxiliary circuit," *IEEE Trans. Ind. Informat.,* vol. 11, no. 1, pp. 64–73, Feb. 2015.

[16] C.-M. Young, S.-F. Wu, W.-S. Yeh, and C.-W. Yeh, "A DC-side current injection method for improving AC line condition applied in the 18-pulse converter system," *IEEE Trans. Power Electron.*, vol. 29, no. 1, pp. 99–109, Jan. 2014.